The generalised vibrational density of states of the metallic glass $Fe_{40}Ni_{40}B_{20}$ determined by neutron inelastic scattering

1989 J. Phys.: Condens. Matter 1 5621

(http://iopscience.iop.org/0953-8984/1/33/005)

J. Phys.: Condens. Matter 1 (1989) 5621–5629. Printed in the UK

The generalised vibrational density of states of the metallic glass $Fe_{40}Ni_{40}B_{20}$ determined by neutron inelastic scattering

R Caciuffo†, O Francescangeli†, S Melone†, M Stefanon‡, E Gering§, J-B Suck§, M Bonnet‖, P Allia¶ and F Vinai††

† Dipartimento di Scienze dei Materiali e della Terra, Università di Ancona, Via Brecce Bianche, I-60131 Ancona, Italy

‡ ENEA, Centro Ricerche Energia 'Ezio Clementel', Bologna, Italy

§ Kernforschungszentrum Karlsruhe, Institut für Nukleare und Festkörperphysik, Karlsruhe, Federal Republic of Germany

‖ Centre d'Etudes Nucléaires Grenoble, Département de Recherche Fondamentale, Grenoble, France

¶ Dipartimento di Fisica, Politecnico di Torino, Torino, Italy

†† Istituto Elettrotecnico Nazionale Galileo Ferraris, Torino, Italy

Received 2 February 1989, in final form 28 April 1989

Abstract. The generalised vibrational density of states $G(\omega)$ has been derived from inelastic neutron scattering measurements for the ternary transition metal–metalloid metallic glass $Fe_{40}Ni_{40}B_{20}$. Two main energy bands are observed centred around 24 and 63 meV and separated by a shallow pseudo-gap near 50 meV. The former band is mainly due to transition metal–transition metal interaction, the latter is associated to localised optical modes involving transition metal–boron bonds. Rather small differences, if any at all, have been observed for samples prepared by the melt spinning technique at different velocities of the rotating wheel. The neutron weighted $G(\omega)$ have been used to calculate thermodynamic quantities like the temperature dependence of the specific heat and of the Debye temperature.

1. Introduction

The $(Fe_{0.5}Ni_{0.5})_{100-x}B_x$ amorphous alloys are among the most frequently studied of all ternary transition metal–metalloid (TM–m) glasses, attracting attention both for scientific and for technological reasons [1]. A number of investigations have been dedicated to the determination of their atomic structure and to the characterisation of their macroscopic properties ([2, 3] and references therein [4–6]). However, little attention has been paid to the atomic dynamics of these systems, despite the fact that the knowledge of the interatomic forces is of fundamental importance for the understanding of the thermodynamics, mechanical and transport properties of a solid. Because of the lack of long-range order, quite a few of the collective excitations in amorphous materials have a localised character in real space and are no longer well defined in momentum space. As a consequence, a description of the atomic vibrations in terms of energy–momentum dispersion relations is often incomplete and the information on the restoring forces must be deduced from the density of vibrational states measured as a function of energy.

Inelastic neutron scattering allows one to measure the double-differential scattering cross section which is directly proportional to the dynamic structure factor of the system and it is therefore the most direct method for such measurements. Pioneering work has been performed by Windsor and co-workers [7] on $Pd_{80}Si_{20}$ and by Suck and co-workers ([8] and references therein) on several metal–metal binary systems [9]. However, only very few investigations of the atomic dynamics of metal–metalloid glasses have so far been published. Recently, Lustig and co-workers have performed a high-resolution investigation of the vibrational properties and the bonding in amorphous $Fe_{78}P_{22}$ and $Ni_{82}B_{18}$ alloys ([10], [11] and references therein). The results obtained by these authors indicate a stronger metallic interaction between Ni–Ni than Fe–Fe, as well as stronger covalent bonds between Fe–P pairs than Ni–B due to a stronger p–d hybridisation.

In this paper we present the scattering amplitude-weighted vibrational density of states $G(\omega)$ obtained by inelastic neutron scattering from $Fe_{40}Ni_{40}B_{20}$ metallic glasses prepared at two different quench rates by the melt-spinning technique. The aim of the experiment was to gain information on the TM–TM and TM–m interactions as well as on the possible dependence of the atomic dynamics on the quench rate. In fact, it is known that several macroscopic physical properties of metallic glasses (and of $(Fe, Ni)_{100-x}B_x$ in particular) are modified by the rate of quenching from the melt, suggesting that samples spun at lower quench rates are somewhat more relaxed toward a structure closer to a free-energy local minimum. The effect is most evident in the case of the magnetic permeability after-effect [12] and of the differential scanning calorimetry signal [13], while the electrical resistivity is significantly, but less strongly influenced [14]. On the other hand, a careful determination of the atomic structure performed on our samples by neutron diffraction failed to detect relevant structural changes, and gives only an indication of a possible reduction of the chemical short-range order parameter with increasing quench velocities [15].

2. Experimental procedure and results

The two $Fe_{40}Ni_{40}B_{20}$ alloys were prepared at the Istituto Elettrotecnico Nazionale Galileo Ferraris, Turin, by melt-spinning at two different velocities of the rotating wheel (30 and 45 m s^{-1}) but otherwise under identical conditions, giving ribbons of about 20 μm thickness, 1 cm width and 7.53 g cm^{-3} mass density.

The ribbons were wound on a Cd frame to obtain 0.6 mm thick planar samples for the neutron experiments. About 8 g of material were illuminated by the neutron beam. Natural boron was used in spite of its high absorption cross section. The absorption corrections are, as a consequence, important but, on the other hand, multiple scattering contributions are considerably reduced.

A high-resolution neutron diffraction study was performed at the UK spallation neutron source, ISIS, in order to characterise the local atomic arrangement. Because the distribution of Fe and Ni atoms on the TM sites in the $Fe_{40}Ni_{40}B_{20}$ is almost random [5], an 'average' TM atom has been considered. The reduced total pair correlation function obtained for the sample spun at 30 m s^{-1} is shown in figure 1. The split first peak, corresponding to the nearest-neighbour distances, allows the determination of the parameters related to the TM–TM and TM–B distributions. In particular, a distance of 2.11(2) Å is found for the TM–B pairs and of 2.54(2) Å for the TM–TM bond. The first nearest-neighbour partial coordination numbers Z may be calculated from the area under the resolved sub-peaks of the radial distribution function, leading to $Z_{TM\text{-}B}$ =

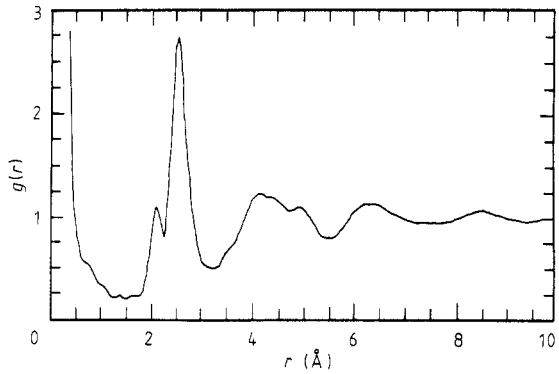

Figure 1. Reduced pair correlation function obtained by neutron diffraction for $Fe_{40}Ni_{40}B_{20}$ amorphous alloy. The split first peak corresponds to the nearest-neighbour coordination shell showing a shorter transition metal–boron than transition metal–transition metal bond.

1.8(2), $Z_{B\text{-}TM} = 7.2(5)$ and $Z_{TM\text{-}TM} = 9.4(9)$. The boron–boron correlation within the first coordination shell is negligible and $Z_{B\text{-}B} \simeq 0$. Very small differences inside the error band are found for other values of the quench rate [15].

The inelastic neutron scattering experiment was carried out using the time-of-flight spectrometer of the Nuclear Research Centre of Karlsruhe at the Melusine reactor in the Nuclear Research Centre, Grenoble, France.

Incident energies E_0 of 30.28 and 121.12 meV were used; by different phasing of a Fermi chopper we selected either the first or the second harmonics in the beam diffracted by a Cu(111) monochromator in transmission geometry.

Scattered neutrons are detected by an array of 296 ^{3}He detectors. They are fixed on a circle of 300 cm radius around the centre of the sample and cover an angular range between $\varphi = 10.48$ and $\varphi = 90.48$ deg. The signals from the detectors are sorted according to the time of flight of the neutron and its scattering angle, so that the scattering cross section can be obtained as a function of energy and momentum transfer $\hbar\omega = \hbar^2(k_0^2 - k^2)/2m$ and $\hbar\boldsymbol{Q} = \hbar(\boldsymbol{k}_0 - \boldsymbol{k})$.

Energy transfers between about 3.5 and 80 meV and momentum transfers between 0.8 and 8 Å^{-1} ($E_0 = 30.28$ meV) were investigated. From the full width at half maximum (FWHM) of the vanadium peak, an energy resolution at zero energy transfer of the order of 7% may be estimated. Besides the sample runs, background and calibration measurements on a vanadium standard were performed. All the measurements were done at room temperature.

The generalised vibrational density of states $G(\omega)$ was calculated following the procedure outlined in [9]. As the samples investigated are coherent scatterers, the dynamic structure factor has to be averaged (for each energy) over all polarisation vectors and over an extended range of the momentum transfer $\hbar\boldsymbol{Q}$. For an amorphous or polycrystalline system this is achieved by taking for each energy transfer the mean value of the one-phonon term of the double-differential cross section weighted with $\sin\varphi$ over the accessible range of scattering vectors [9]:

$$G(\omega) = \frac{4\pi}{\sigma_c}\frac{K_0}{K}\hbar\omega(1 - e^{-\beta})\frac{8MKK_0}{\hbar^2(Q^4_{max} - Q^4_{min})} \times \int_{\varphi_{min}}^{\varphi_{max}} \exp(2W(Q))\left(\frac{d^2\sigma}{d\Omega\, dE}\right)_{1ph} \sin\varphi\, d\varphi \qquad (1)$$

where σ_c is the coherent cross section, $\beta = \hbar\omega/K_BT$ with K_B the Boltzmann constant

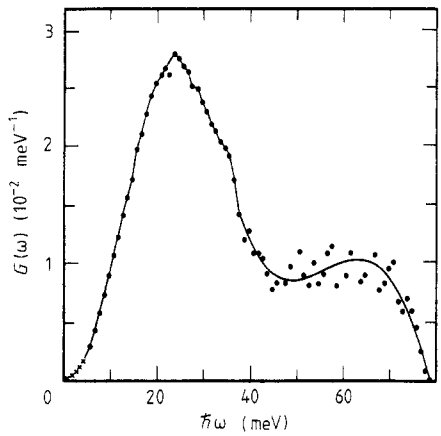

Figure 2. Generalised vibrational density of states measured for a sample of $Fe_{40}Ni_{40}B_{20}$ melt-spun at 30 m s^{-1}. The full curve is a polynomial fit to the experimental data. The first five values up to about 5 meV (×) are extrapolations according to $G(\omega)\alpha\omega^{3/2}$.

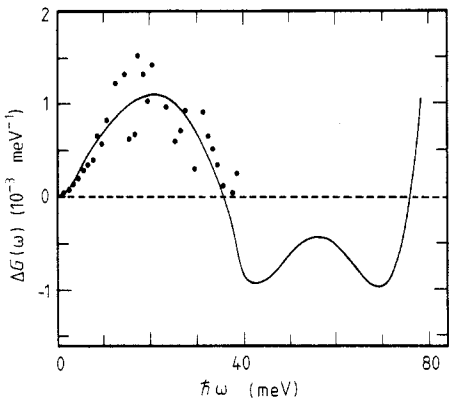

Figure 3. Difference between the frequency distributions obtained for samples spun under identical conditions but different quenching rates, namely 45 m s^{-1} and 30 m s^{-1}, respectively.

and $\exp[-2W(Q)]$ is the Debye–Waller factor. The generalised density of states $G(\omega)$ is related to the weighted sum of the partial distributions $g_i(\omega)$ of each element i in the sample according to

$$G(\omega) = \sum_i \exp[-2W_i(Q)]\frac{\sigma_c^i}{M_i} g_i(\omega) \Big/ \sum_i \exp[-2W_i(Q)]\frac{\sigma_c^i}{M_i} \tag{2}$$

M_i and σ_c^i being the mass and the bound coherent scattering cross section of atoms of type i ($\sigma_c^{Fe}/M_{Fe} = 0.21$ b, $\sigma_c^{Ni}/M_{Ni} = 0.30$ b, $\sigma_c^{B}/M_B = 0.46$ b).

To calculate the $G(\omega)$ from (1), the contributions of multiphonon processes to the measured intensities must be removed. This was performed in the harmonic and incoherent approximation by an iterative procedure [9] starting from the measured cross section as zeroth approximation.

The frequency distribution obtained for the sample spun at 30 m s^{-1} from the neutron energy gain spectra at an incident energy of 30.28 meV is shown in figure 2. The data are normalised to

$$\int_0^{\omega_{max}} G(\omega)\,\mathrm{d}\omega = 1. \tag{3}$$

The first five values, up to about 5 meV, are calculated assuming [16] $G(\omega)\alpha\omega^{3/2}$ (a fit of the data on a double logarithmic scale in the range between 5 and 10 meV gives a slope of 1.46. On the other hand, the extrapolation to zero energy with the help of a Debye spectrum would produce an unphysical kink). The full curve above 40 meV is a fit of the experimental data to a polynomial function. Ten terms have been included in the multiphonon correction with an effective mass $M^* = 43$, giving an average relative deviation of the order of 10^{-4} at the fourth iteration. Good agreement is obtained with the spectrum calculated from the data collected for the same sample with an incident energy of 121.12 meV.

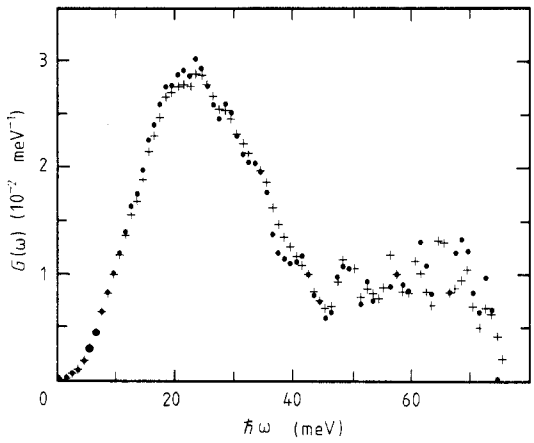

Figure 4. Comparison between the frequency distributions obtained: full circles, using the whole detector bank; crosses using the higher angle detectors only. No appreciable differences are observed, showing that inelastic magnetic scattering effects are negligible.

Figure 3 shows the difference between the generalised frequency distributions $G(\omega)$ of the samples spun at 45 m s^{-1} and 30 m s^{-1}, respectively. The full curve is a polynomial fit to the experimental data. The compensation of the negative values above 36 meV stems from the fact that both vibrational density of states were normalised to 1 at the same cut-off frequency (ω_{max} = 80 meV). The results seem to suggest a small enhancement of the low energy band in $G(\omega)$ as the rate of quenching is increased; however, one has to note the change of scale by an order of magnitude on going from figure 2 to figure 3.

Since neutron measurements were performed at room temperature with the samples in the magnetically ordered state (T_c = 668 K), the probable presence of inelastic magnetic scattering must be considered. Magnetic and vibrational scattering may be distinguished by their different dependences on the neutron momentum transfer, Q. The former falls in intensity with Q as the square of the magnetic form factor $f(Q)$, the latter increases in intensity with Q. In order to verify if our derivation of the vibrational density of states is affected by the presence of inelastic magnetic scattering, calculations were then repeated using data from the high-angle detector bank only. The range covered in this case is between about 64 and 90 deg and magnetic scattering is negligible. Assuming in fact the form factor for Fe^{3+} ions [17], with an incident energy of about 30 meV and a full scattering angle of 80 deg, $f^2(Q)$ has a value of about 0.05 for $\hbar\omega$ = 20 meV and 0.01 for $\hbar\omega$ = 60 meV (a still more favourable situation occurs for the E_0 = 121 meV run). The results are compared in figure 4 with the frequency distribution obtained using the whole angular range. No appreciable differences are observed, showing that magnetic effects are too small to be detected in the present experiment.

3. Discussion

In contrast to metal–metal amorphous systems where normally a single low-energy band is observed [8], the vibrational density of states of $Fe_{40}Ni_{40}B_{20}$ consists of two broad peaks, centred at about 24 meV and 63 meV, respectively.

This result is qualitatively similar to those obtained for other TM–m binary systems both from experiments [7, 10, 11] and theoretical models [18]. In particular, in [18] the vibrational spectrum of $Fe_{100-x}P_x$ amorphous system is calculated by the recursion method and it is shown to consist of a low-energy band, mainly associated with the

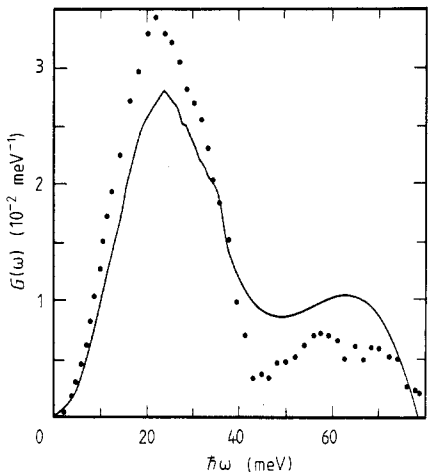

Figure 5. Comparison between the spectra obtained by inelastic neutron scattering: full curve, for $Fe_{40}Ni_{40}B_{20}$; full circles, for $Ni_{82}B_{18}$ amorphous alloy (from [10]). The areas under the two curves are normalised at the same cut-off frequency.

vibrational modes around Fe atoms, and of a higher energy band mainly arising from vibrations around P atoms. In our case, the Fe and Ni atoms may be considered to substitute each other randomly over the TM sites. Moreover, the coordination number Z_{TM-TM} is almost five times Z_{TM-B} so that the low-energy band is considered to be predominantly caused by TM–TM interactions. On the other hand, Z_{B-B} being almost zero, the higher energy band results essentially from TM–B bonds.

Further comparisons with the results of [18] suggest that the high-frequency peak corresponds to localised optical vibrational modes of the TM–B–TM colinear chains, while the low-frequency peak should be associated to the acoustic modes. In particular, the main feature could arise from the transverse mode corresponding to the propagation of shear modes and the shoulder visible at about 32 meV could be due to the longitudinal mode determined by the forces restoring the volume changes.

The generalised vibrational density of states obtained in the present work is compared in figure 5 with the spectrum measured for the $Ni_{82}B_{18}$ amorphous alloy [10], after normalisation to the same cut-off frequency ω_{max}. Taking into account the different neutron weighting factors to be used in (2), the results compare favourably. The positions of the energy-band maxima are almost the same, but the statistical accuracy of our data is insufficient at energy transfers above 45 meV to resolve the fine structure observed in the high-energy peak of $Ni_{22}B_{18}$. In that case, two features with maxima at 56 and 68 meV are present while only a broad peak centred about 63 meV can be defined from the present experiment on $Fe_{40}Ni_{40}B_{20}$.

Assuming, in a simple model, a force constant given by $K = m_r E^2$ (where m_r is the reduced mass of the interacting atoms and E is the energy of the maximum in the corresponding vibrational band) one obtains $K_{TM-TM} \sim 0.46\, K_{TM-B}$. This indicates a stronger TM–m than TM–TM interaction, as already suggested by the shorter values of the TM–B bond.

Figure 3 shows that the intensity of the TM–TM band is slightly higher in the sample spun at 45 m s^{-1}. The observed enhancement corresponds to a decrease of about 4% of the second moment $\langle\omega^2\rangle$ of the frequency distribution $G(\omega)$, a parameter representing some mean force constant in the sample. This fact could indicate a softening of atomic bonds due to larger atomic volumes, but no structural modifications are seen in the neutron diffraction study and the packing efficiency in the glass does not appear to be

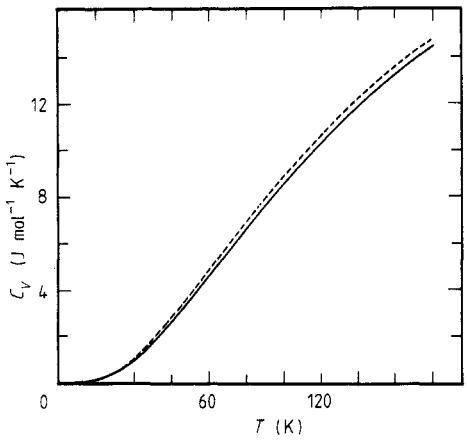

Figure 6. Temperature dependence of the vibrational part of the specific heat at constant volume calculated from the generalised frequency distribution of $Fe_{40}Ni_{40}B_{20}$ samples melt-spun at: broken curve, 45 m s^{-1}; full curve, 30 m s^{-1}.

influenced by the rate of quenching. On the other hand, a small change in the chemical short-range order could occur with an enhanced probability for a TM atom to have similar neighbours when the quench rate is increased [15]. As a consequence, an enhancement of the low-frequency band associated with TM–TM interactions should occur. However, the observed differences are rather small and unambiguous conclusions cannot be reached in absence of a rigorous and reliable error analysis.

In order to estimate the effects of the observed variations on the thermodynamic properties of the $Fe_{40}Ni_{40}B_{20}$ metallic glass, the scattering amplitude weighted frequency distributions $G(\omega)$ (which are normally only good approximations to the real vibrational density of states) have been used to calculate the Debye temperature $\theta_D(T)$ and the temperature dependence of the vibrational part of the specific heat $C_v(T)$ at constant volume, according to

$$C_v(T) = 3R\int_0^{\beta_{max}(T)} \frac{G(\beta)\beta^2\,e^{-\beta}}{(1-e^{-\beta})^2}\,d\beta \tag{4}$$

$$\theta_D(T) \simeq \theta_D(\infty)\{1 - A[\theta_D^2(\infty)/T^2] + B[\theta_D^4(\infty)/T^4]\}^{1/2} \tag{5}$$

where $G(\beta) = K_B T G(\omega)$, R is the gas constant and [19]

$$\theta_D(\infty) = (\tfrac{5}{3}\langle\omega^2\rangle)^{1/2}$$

$$A = (3/100)[\langle\omega^4\rangle/\langle\omega^2\rangle^2 - 25/21] \tag{6}$$

$$B = (1/1400)[\langle\omega^6\rangle/\langle\omega^2\rangle^3 - 125/81 - 100A]$$

the symbol $\langle\ \rangle$ indicating a $G(\omega)$-weighted average.

The specific heat obtained for the $Fe_{40}Ni_{40}B_{20}$ samples spun at 30 and 45 m s^{-1} are shown in figure 6. Due to the energy resolution of the experiment, data below 35 K should be considered as being qualitative.

A small difference between the two samples may be observed, but we are not able to assign a reliable error band to the calculated curves, because of the many approximations involved. We cannot affirm, as a consequence, that this difference has a physical origin, even though the trend is consistent with the results of macroscopic

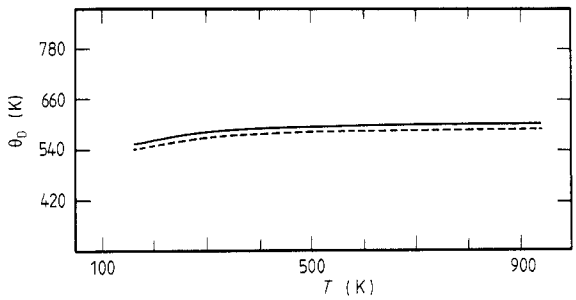

Figure 7. Temperature dependence of the Debye temperature $\theta_D(T)$ for samples melt-spun at: broken curve, 45 m s^{-1}; full curve, 30 m s^{-1}.

measurements at high temperature [14]. A similar situation occurs for the Debye temperature, reported in figure 7. An almost constant behaviour is observed with a difference of the order of 2% between the two samples ($\theta_D(\infty) = 595$ K for $v = 30$ m s^{-1} and $\theta_D(\infty) = 582$ K for $v = 45$ m s^{-1}).

In conclusion, we have measured the generalised vibrational density of states for the ternary $Fe_{40}Ni_{40}B_{20}$ metallic glass by inelastic neutron scattering experiments.

The results are in agreement with previous theoretical and experimental works on binary metal–metalloid glasses. The frequency distribution consists of two bands, the lower associated with acoustic modes and transition metal–transition metal interactions, the upper one with localised optical modes involving transition metal–metalloid bonds. The measured frequency distribution has been used to estimate the temperature dependence of the specific heat at constant volume and of the Debye temperature. Small differences have been observed for samples prepared by melt spinning under identical conditions but different quench velocities. In fact, by reducing the rate of the melt quenching process relaxation phenomena are expected to occur which should be accompanied by modifications in both the local order and the vibrational dynamics of the glass. Moreover, the quenching conditions could influence the density of defect regions where low-energy excitations are enhanced. However, only rather small differences are revealed both by neutron diffraction (structural study) and neutron inelastic scattering (dynamics study), even though a large dependence on the quench rate has been observed for a number of macroscopic properties of the investigated system.

Further neutron experiments are planned on simpler metallic glasses, prepared with considerably larger differences in the quench velocities, in order to address the problem of the dependence on the quenching conditions of the vibrational properties of amorphous alloys.

Acknowledgments

It is a pleasure to thank Professor F Rustichelli for many useful discussions during the preparation of this work and for critical reading of the manuscript. The collaboration of Drs W S Howells and A K Soper in the diffraction experiments is gratefully acknowledged.

References

[1] Fournier P 1984 *Les Amorphes Metalliques (Ecole d'Hiver d'Aussois)* (Paris: Editions de Physiques) p 595

[2] Wong J 1981 *Springer Topics in Applied Physics* vol 46, ed. H-J Güntherodt and H Beck (Berlin: Springer) p 45
[3] Steeb S and Lamparter P 1984 *J. Non-Cryst. Solids* **61/62** 237
[4] Thijsse B J and Majewska-Glabus I 1985 *Rapidly Quenched Metals* ed. S Steeb and H Warlimont (Amsterdam: Elsevier) p 435
[5] Sietsma J and van Dijk C 1985 *Rapidly Quenched Metals* ed. S Steeb and H Warlimont (Amsterdam: Elsevier) p 463
[6] Svàb E, Bellisant R and Mèszàros Gy 1985 *Rapidly Quenched Metals* ed. S Steeb and H Warlimont (Amsterdam: Elsevier) p 467
[7] Windsor C G, Kheyrandish H and Narasimhan M C 1979 *Phys. Lett.* **70A** 485
[8] Suck J-B, Rudin H, Güntherodt H-J and Beck H 1981 *J. Phys. C: Solid State Phys.* **14** 2305
[9] Suck J-B and Rudin H 1983 *Springer Topics in Applied Physics* vol 53, ed. H Beck and H-J Güntherodt (Berlin: Springer) p 217
[10] Lustig N, Lannin J S, Price D L and Hasegawa R 1985 *J. Non-Cryst. Solids* **75** 277
[11] Lustig N, Lannin J S, Carpenter J M, Arai M and Hasegawa R 1985 *Rapidly Quenched Metals* ed. S Steeb and H Warlimont (Amsterdam: Elsevier) p 501
[12] Allia P and Vinai F 1982 *Phys. Rev.* B **26** 6141
[13] Altounian Z 1987 *Magnetic Properties of Amorphous Metals* ed. A Hernando, V Madurga, M C Sanchez-Trujillo and M Vasquez (Amsterdam: Elsevier) p 80
[14] Allia P, Sato-Turtelli R, Vinai F and Riontino G 1982 *Solid State Commun.* **43** 821
[15] Caciuffo R, Stefanon M, Howells W S, Soper A K, Allia P, Vinai F, Melone S and Rustichelli F 1989 *Physica* B **156–157** 220
[16] Suck J-B, Rudin H, Güntherodt H-J, Beck H, Daubert J and Gläser W 1980 *J. Phys. C: Solid State Phys.* **13** L167
[17] Boucherle J X 1984 *Compilation of Magnetic Form Factors and Magnetisation Densities* (Grenoble: Neutral Diffraction Commission, CEN)
[18] Ishii Y and Fujiwara T 1980 *J. Phys. F: Met. Phys.* **10** 2125
[19] Barron T M K, Berg W T and Morrison J A 1957 *Proc. R. Soc.* A **242** 478